PROCEEDINGS OF SCIENCE

paolo.persi@inaf.it mt@astro.unam.mx

A infrared study of high mass star forming regions

Paolo Persi[a,*] **and Mauricio Tapia**[b]

[a] *INAF Istituto Astrofisica e Planetologia Spaziale, Roma, Italy*

[b] *UNAM University Nacional Autonoma de Mexico, Ensenada, Mexico*

In this paper we discuss the importance of the infrared observations from the near-IR to millimeter wavelengths of high mass star forming regions. In particular we present the infrared observations of three of these regions.

Frontier Research in Astrophysics – IV (FRAPWS2024)
9-14 September 2024
Mondello, Palermo, Italy

*Speaker

 ISSN 1824-8039 . Published by SISSA Medialab.

PoS(FRAPWS2024)020

Table 1: Sample of the observed high-mass protostars

IRAS	α(2000)	δ(2000)	D	L
	h m s	∘ ′ ″	Kpc	$L_\odot$
IRAS 12127-6244	12 15 23.9	-63 01 20	10.8	1830×10^3
IRAS 13395-6153	13 43 02.1	-62 08 52	5.3	277×10^3
IRAS 16112-4943	16 15 01.3	-49 50 37	3.3	774×10^3

1. Introduction...

The formation of massive stars (OB stars with masses greater than 8 $M_\odot$) in our Galaxy is quite complex and requires good observational knowledge about star-forming environments. Theoretically, a massive proto-stellar embryo heats and eventually ionizes the gas of its surrounding envelope, creating an HII region which develops by expanding within the cloud. A review of high-mass star and massive cluster formation in the Milky Way based on the recent surveys in the far- infrared (Herschel/Hi-GAL) , mid-IR (Spitzer/GLIMPSE) and sub-millimeter (ATLASGAL) has been reported by [1].
Observations at different wavelengths from near and far-IR of three high mass star forming regions are discussed here in order to track a possible evolutionary model of high mass star formation. The list of the observed regions is reported in Table 1.

2. Observations

2.1 Near-IR images and spectroscopy.

Near-infrared images of the selected star forming regions of Table 1 were obtained through standard broad-band JHKs filters as well as through narrow-band H_2 (λo = 2.122 μ, $\Delta\lambda$ = 0.024μ) and Br γ (λo = 2.165 μm, $\Delta\lambda$= 0.022μ filters, using the Perssons Auxiliary Nasmyth Infrared Camera (PANIC) attached to the Magellan Baade 6.5 m telescope at Las Campanas Observatory (Chile). PANIC uses a Hawaii 1024 × 1024 HgCdTe array that provides a 120arcsec×120arcsec field of view with a scale of 0.125arcsec/pix [2]. We obtained nine dithered frames, each of 60, 40 and 20 s effective integration time in J, H, Ks, respectively, and 60 s in the narrow-band filters, by offsetting the telescope by 6arcsec between consecutive exposures. The mean measured full width at half-maximum (FWHM) point spread function (PSF) in Ks was about 0.5arcsec.
Near-IR spectroscopy was obtain for the source IRAS 12127-6244 using the Folded-port Infrared Echellette Spectropraph (FIRE) in its high throughput prism mode. This configuration provides simultaneous spectra from 0.82 to 2.51μ with spectral resolutions R_J = 500, R_H = 450 and R_K = 300 in the J, H, K_s atmo- spheric windows. The instrument is described in detail by [3]

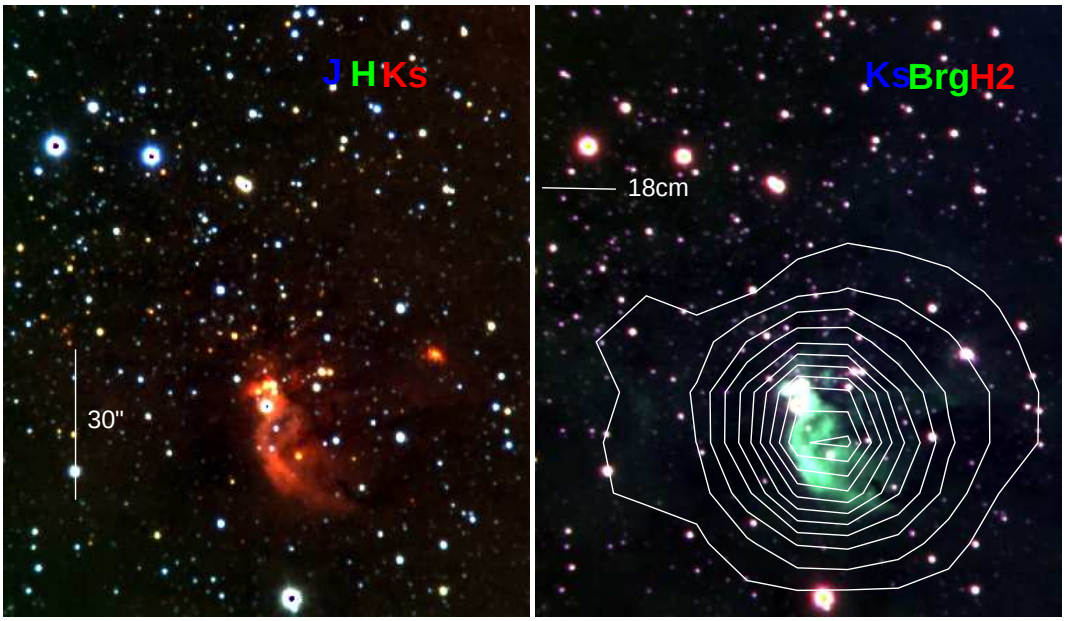

Figure 1: *Left panel:*Color-composed image of IRAS 12127-6244 obtained with the J (blue), H(green) and Ks ,(red) filters.*Right panel:* Color-composed image of IRAS 12127-6244 obtained with Ks(blue),Br γ (green), H_2 red filters. The contours show the HII region observed at 18cm.

2.2 SPITZER archive images.

Flux calibrated mid-IR images at 3.6, 4.5, 5.8 and 8 μm of the star forming regions of Table 1 where obtained from the Spitzer Galactic Legacy Infrared Mid plane Survey Extraordinaire key program survey ([4], [5]) .

2.3 HERSHEL, HI-GAL images

Far-infrared images at 70, 160, 250, 350 and 500 μm have been obtained as part of the Herschel Hi-GAL survey. The images were reduced using the HI-GAL standard pipeline [6] , and source extraction and photometry was performed using the Curvature Threshold Extractor package (CuTEx,[7]) independently at each band.
The images and the photometry of the sources of Table 1 will be discussed in the next sections.

3. Discussion

3.1 IRAS 12127-6244

MId-IR , sub-millimeter, millimeter and radio observations of this region obtained by ([8], [9], [10], [11]) have shown that IRAS 12127-6244 is a high mass star forming region.
Fig.1 show the color-composed JHKs image (Left panel) and the Ks,Br γ H_2 image (Right panel) of IRAS 12127-6244. Around the IRAS position a red nebulosity is observed with an extended ,Br γ emission in agreement with the presence of a giant HII region .

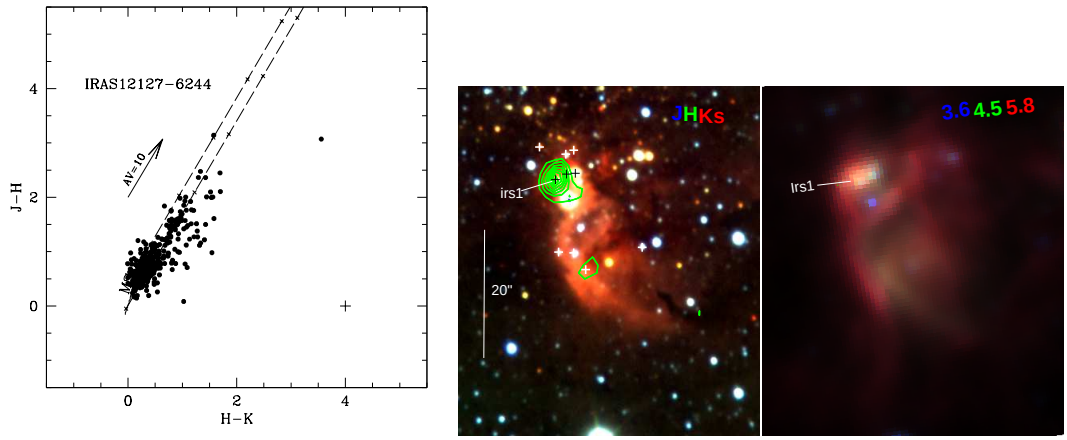

Figure 2: *Left panel:* J-H versus H-Ks diagram of all sources measured in JHKs with uncertainties less than 0.15mag in each filters.*Central panel:*color-coded JHKs image around the red nebulosity. The contours show the radio source detected at 6cm, while the symbol + indicate the sources with near-IR excess.*Right panel:* Color-composed Spitzer image obtained with the 3.6 (blu), 4.5(green) and 5.8 (red)μm images.

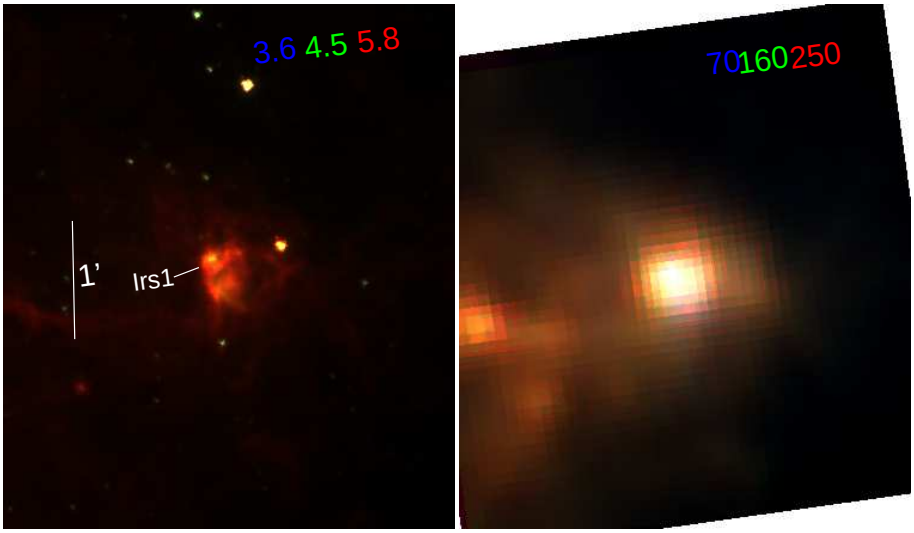

Figure 3: Comparison between the color-coded Spitzer image and the color coded HI-GAL image of IRAS 12127-6244.

A very accurate photometry was obtained in a field of 120 arcsec ×120 arcsec around the IRAS position. The J-H vs H-Ks diagram of Fig.2(Left panel) show the presence of several sources with IR excess. Many of these sources with IR excess are located inside the red nebulosity as shown in Fig.2 (Central panel).This indicate that a young stellar cluster is present in the region. One of these source(Irs1), at the position $\alpha(2000) = 12^{h}\ 25^{m}\ 25^{s}$, $\delta(2000) = -63^{\circ}\ 01'\ 17.35''$, is coincident with the radio source detected at 6cm [11], with the 10.4 μm source detected by [8] and with a Spitzer source (see Fig.2 Right panel). Irs1 is also detected in the five filters of HI-GAL survey as reported in Fig.3.

The observed near-IR spectrum of Irs1 is dominated by Bracket lines as shown in Fig.4 (Right

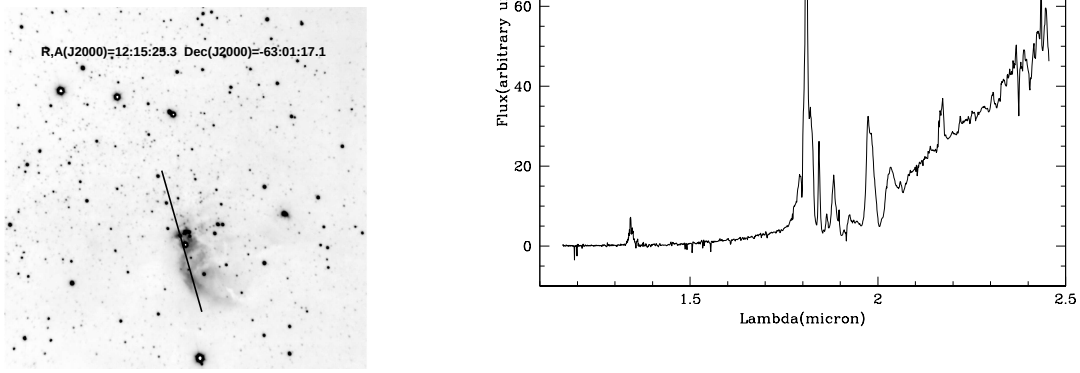

Figure 4: *Left panel:* Slit position of the near-infrared spectrum of Irs1 *Right panel:* Spectrum of Irs1 between 0.82 to 2.51μ

panel). All these observations indicate that the source is a high massive star at very early evolutionary stage. Combining the observations at the different wavelengths, we have obtained the spectral energy distribution (SED) that will be discussed in the next section.

3.2 IRAS 13395-6153 (AFGL 4176)

The presence of Methanol maser [14], water maser [15], 1.2mm emission [10], radio continuum [16] and the infrared observations between 1.25 and 20 μm obtained by [17], indicate that this region identified also as AFGL4176, is a high mass star forming region. The color-coded JHKs image reported in Fig.5(Left panel) show the presence of a red nebulosity around the IRAS position with at the center a very bright near-IR source, while the color-coded Ks,Br γ H_2 image (Fig.5 Right panel) indicate the presence of Br γ emission in agreement with the observed radio emission at 18cm .

The infrared photometry obtained in a field of 30arcsec×30arcsec around the IRAS position show the presence of a number of star with IR excess as reported in the J-H versus H-Ks diagram of Fig.6(Left panel). This indicate that a cluster of young stellar objects is associated with the IRAS source(Fig6 Right panel). In addition IRAS 13395-6153 show an near-IR excess and is coincident with a Spitzer and HI-GAL source as shown in Fig.7.

3.3 IRAS 16112-4943

IRAS 16112-4943 is associated with a giant HII region ([16]) , methanol maser ([14]) , OH maser ([18]) and 1.3mm emission [10]. Our near-IR images in the broad band and narrow band filters show the presence of extended nebulosity associated to the radio continuum as shown in

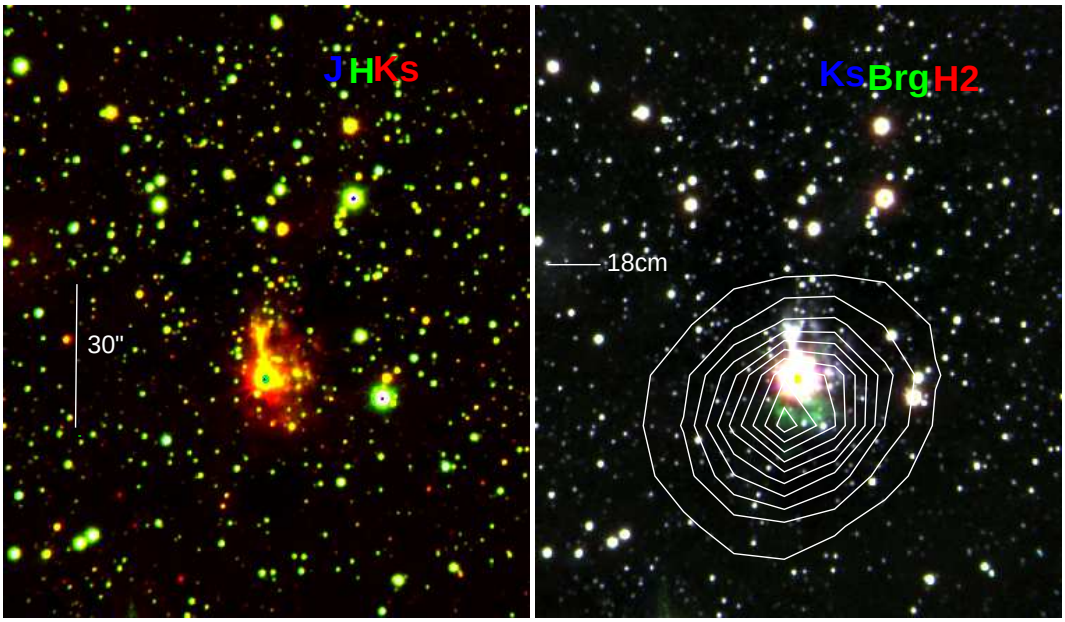

Figure 5: *Left panel:*Color-composed image of IRAS 13395-6153 obtained with the J (blue), H(green) and Ks ,(red) filters.*Right panel:* Color-composed image of the same region obtained with Ks(blue),Br γ (green), H_2 red filters.The contours show the HII region observed at 18cm

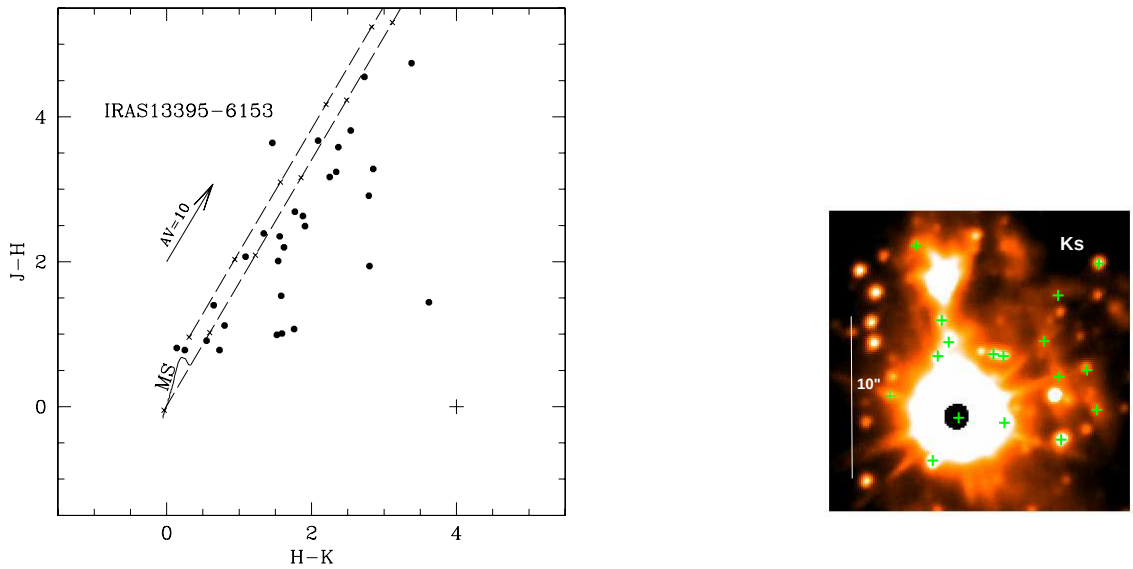

Figure 6: *Left panel:* J-H versus H-Ks diagram of sources measured in JHKs in a field of 30 arcsec ×30 arcsec around IRAS 13395-6153 in each filters..*Right panel:* Ks image around the IRAS position.The symbol + indicate the sources with near-IR excess.

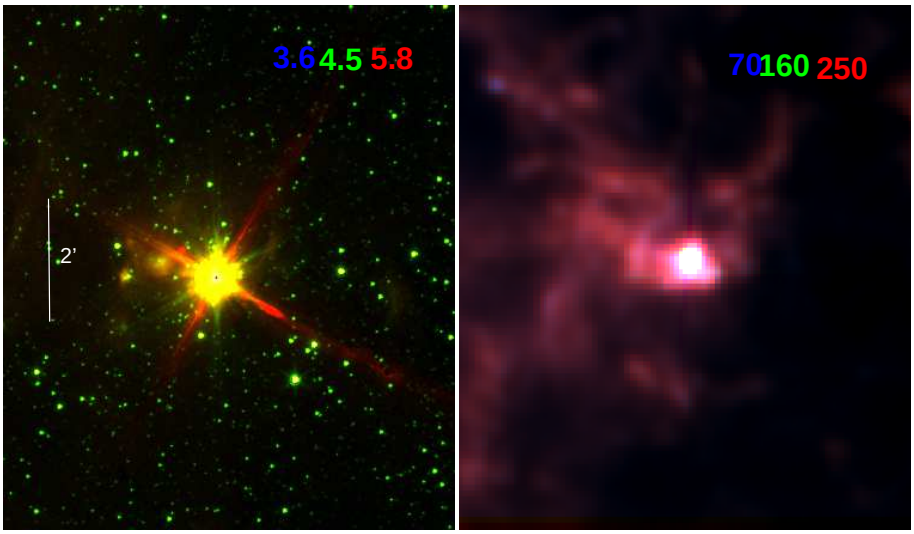

Figure 7: Comparison between the color-coded Spitzer image and the color-coded HI-GAL image of IRAS 13395-6153.

Fig.8.
Two star forming regions are associated with this area as show the color-coded Spitzer image and the 70μm contour derived from the Hi-GAL image (Fig.9). The region I is coincident with the IRAS source, while the region II lie along a diffuse emission. For both the regions we have obtained the spectral energy distribution discussed in the next section.

4. Spectral energy distribution (SED)

Combining the observations at different wavelengths we have derived the spectral energy distribution (SED) of the very young stellar sources here analyzed. The SEDs reported in Fig.10 have been fitted with the in falling envelope + disc + central source radiation transfer model described by [12] using a fitting tool of [13]. As an example we report in Table 2 the derived parameters for the high mass young stars IRAS 12127-6244(Irs1) and IRAS 13395-6153.

5. Conclusion

In this paper we have shown the important role of the infrared observations at different wavelengths relative to the analysis of star forming regions. The analysis of three regions including high resolution near-IR , SPITZER and HI-GAL images have permit to identify the high mass young stellar objects(HMYSOs) and to derive the parameters relative to these sources.In addition a cluster of very young star is present around these HMYSOs.

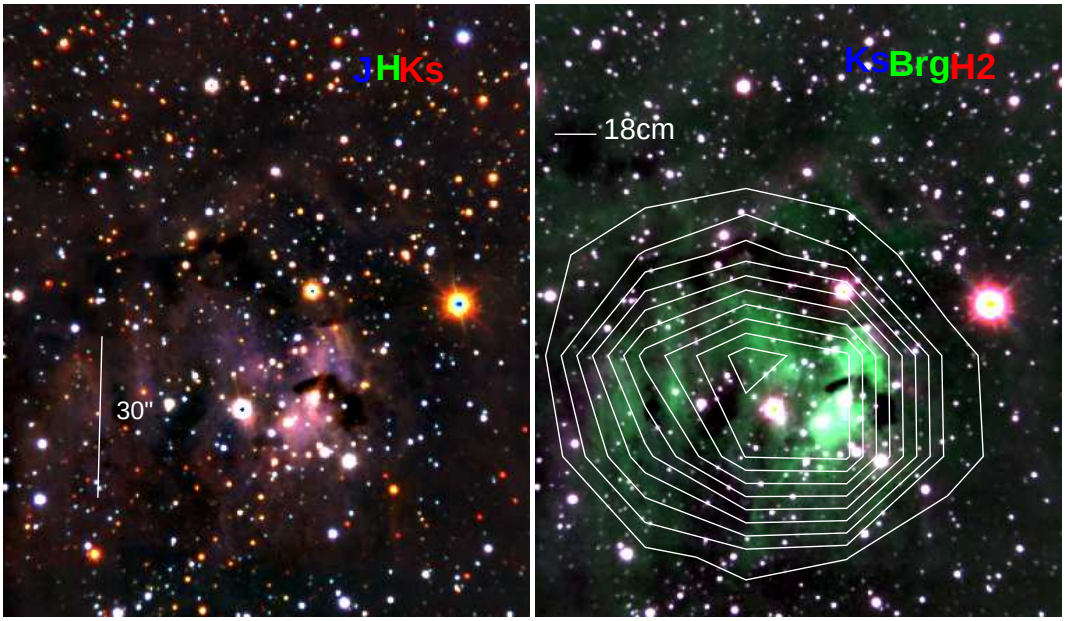

Figure 8: *Left panel:*Color-composed image of IRAS 16112-4943 obtained with the J (blue), H(green) and Ks ,(red) filters.*Right panel:* Color-composed image of the same region obtained with Ks(blue),Br γ (green), H_2 red filters.The contours show the HII region observed at 18cm

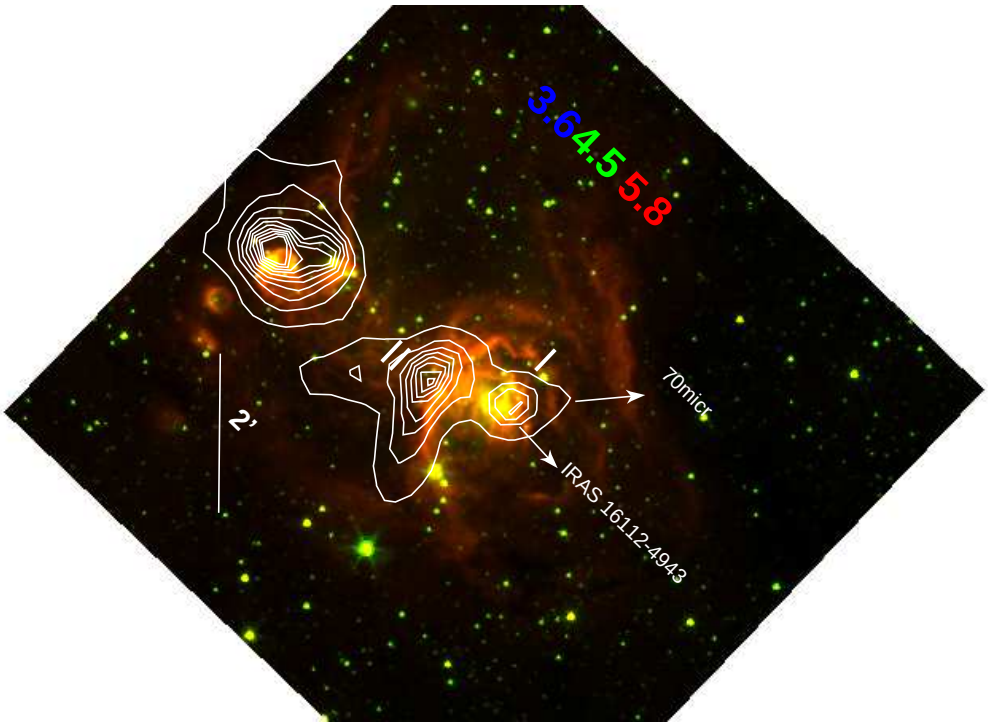

Figure 9: Color-coded Spitzer image obtained with the 3.6 (blu), 4.5(green) and 5.8 (red)μm images .The contour show the HI-GAL image at70μm .

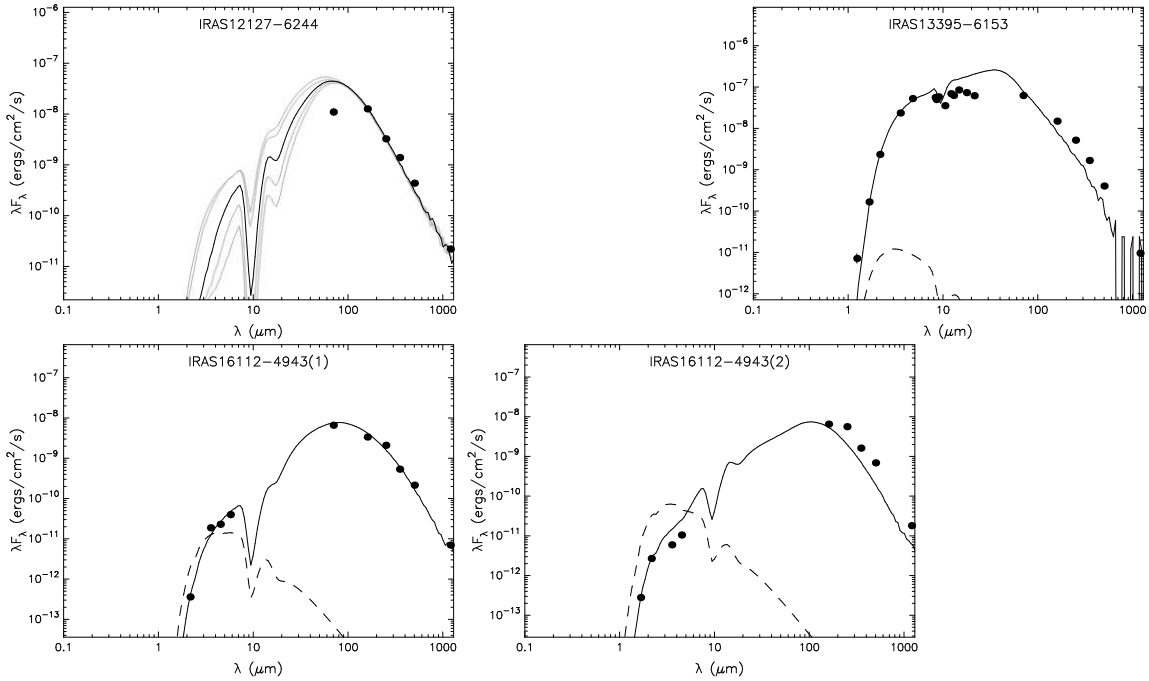

Figure 10: Spectral energy distributions (SED)of the high mass young stars here discussed.

Table 2: Physical parameters from model fit [13] to SEDs.

Parameters	IRAS12127-6244(Irs1)	IRAS13395-6153
Stellar mass (Msun)	14.7	48.2
Stellar temperature (K)	17000	30000
Envelope accretion rate (Msun yr$^-$1)	8.8×10^{-3}	2.0×10^{-5}
Disc mass (Msun)	1.5×10^{-2}	4.0×10^{-4}
Disc accretion rate (Msun yr$^-$1)	2.6×10^{-1}	3.9×10^{-4}
Inclination angle (degrees)	23.6	31.8
A_V (magnitudes)	45	36
$L_{\rm bol}$ ($L_\odot$)	5.8×10^4	3.5×10^5

References

[1] Motte,F.,Bontemps,S.,Louvet,F.,2018.,*ARA&A* 56:41-82

[2] Martini P., Persson S.E., Murphy D.C., et al., 2004 Proc.SPIE 5492 1653

[3] Simcoe R.A., et al 2013 *PASP* 125 270

[4] Benjamin R.A., et tal., 2003 *PASP* 115 953

[5] Churchwell E., et al., 2009 *PASP* 121 213

[6] Traficante, A., Calzoletti, L., Veneziani, M., et al. 2011, *MNRAS* 416 2932

[7] Molinari S., Schisano E., Faustini F., et al., 2011, *A&A* 530 A133

[8] Mottram J C., et al., 2011, *A&A* 530 A133

[9] Molinari S., Pezzuto S., Cesaroni R., et al., 2008, *A&A* 481 345

[10] Beltran M.T., Brand J., Cesaroni R., et al., 2006, *A&A* 447 221

[11] Urquhart J.S., Busfield A L.,, Hoare M.G., et al., 2007, *A&A* 461 11

[12] Robitaille T.P., Whitney B.A., Indebetonw R., et al., 2006, *ApJS* 167 256

[13] Robitaille T.P., Whitney B.A., Indebetonw R., et al., 2007, *ApJS* 169 328

[14] Pestalozzi M.R, Minier V., Booth R.S., et al., 2005, *A&A* 432 737

[15] Breen S.L., Caswell J.L., Ellingson S.P., et al. 2010, *MNRAS* 406 1847

[16] Ellingson S.P., Shabala S.S.,Kurtz S.E., et al. 2005, *MNRAS* 357 1003

[17] Persi,P., Ferrari-Toniolo M.,Spinoglio L., et al., 1986, *A&A* 157 29